Spectrochimica Acta Part A: Molecular and Biomolecular Spectroscopy 253 (2021) 119568

Contents lists available at ScienceDirect

Spectrochimica Acta Part A: Molecular and Biomolecular Spectroscopy

journal homepage: www.elsevier.com/locate/saa

# Monitoring UV-accelerated alteration processes of paintings by means of hyperspectral micro-FTIR imaging and chemometrics

M. González-Cabrera, A. Domínguez-Vidal, M.J. Ayora-Cañada *

*Department of Physical and Analytical Chemistry, Universidad de Jaén, Campus Las Lagunillas, s/n, 23071 Jaén, Spain*

## HIGHLIGHTS

- FTIR hyperspectral microimaging to monitor alteration of organic binders in paintings.
- UV exposition induced both spectroscopic and color changes through ageing.
- PCA models to detect degradation trends depending on the pigment-binder interaction.
- Processes as binder evaporation and oxidation of proteins and lipids noticed.

## GRAPHICAL ABSTRACT

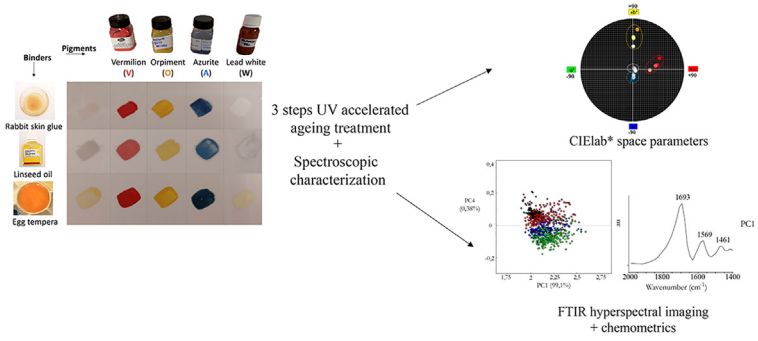


## ARTICLE INFO

*Article history:*
Received 23 October 2020
Received in revised form 26 January 2021
Accepted 28 January 2021
Available online 9 February 2021

*Keywords:*
Hyperspectral imaging
FTIR microspectroscopy
Accelerated UV ageing
PCA
Degradation of organic binders
Colored pigments

## ABSTRACT

We explored the potential of infrared hyperspectral microimages to investigate the alteration of organic binders in pictorial layers after artificial UV light ageing. A set of paint mockups was prepared considering three different binders, namely, rabbit glue (a collagen-based proteinaceous binder), linseed oil (representative of drying oils) and egg tempera (a mixture of egg yolk and linseed oil). Four pigments (vermilion, orpiment, azurite and lead white) were considered in order to investigate the influence of pigment-binder interaction, following color changes by means of fiber optic reflectance spectroscopy (FORS). FTIR micro-images provided a representative picture of the complex and heterogeneous structure of paintings since each pixel contained the whole spectrum of the sample area from it was recorded. Principal component analysis (PCA) was used to analyze the FTIR images data in order to extract useful information about spectral changes taking place during UV induced ageing.

Significant trends were observed, mainly depending on the binders and their degradation as a consequence of UV exposition in this pilot study on model samples. Several processes, such as the oxidation of proteins with the formation of carbonyl moieties and changes in amide band positions have been detected in the case of rabbit skin glue. The evaporation of linseed oil, probably due to the breakdown of the triacylglycerols, has been noticed for the binder alone but not when it was mixed with the pigments. In these cases, other spectral features depending on the pigment have been observed in the loading plots upon oxidation, namely the broadening of the carbonyl band, the appearance of carboxylic and dicarboxylic acids and the formation of metal carboxylates. For egg tempera, the main changes detected were related to the oxidation of lipidic components present in egg yolk fraction. Furthermore, in this case, the trend observed in the score graphs suggested that the presence of lead white accelerates its oxidation. It is interesting to note the major stability of the colored pigments when using this binder.



* Corresponding author.
*E-mail address:* mjayora@ujaen.es (M.J. Ayora-Cañada).

https://doi.org/10.1016/j.saa.2021.119568
1386-1425/

## 1. Introduction

Heritage science is, nowadays, a well-established multidisciplinary field as the scientific study of cultural heritage artefacts can provide a deeper knowledge of the origin, age, sort of fabrics or even social status of the time [1]. The field is in continuous expansion due to the development of new instrumentation and methods for investigation of artworks, stimulated by the rapid progress in physics, chemistry and computer technology. Solving problems through scientific inquiry is one of the basis of cultural heritage conservation [2,3]. Thus, the analysis of alteration mechanisms in artworks is notably relevant for conservation and restoration procedures, because its understanding can aid to make strategic decisions on their long-term preservation [4–6].

Several factors can influence the wear of the layers of the paintings, such as the support, the preparation layers, and the mixture of binder and pigment, among others. Either natural or anthropogenic agents, like extreme temperature or humidity conditions [7,8], chemical reactions between binders and pigments [9], the presence of small bugs, micro-organisms [10], dust or a not careful treatment, can damage the physical state and chemical composition of the artwork [11]. Prolonged exposure to an ultraviolet (UV) radiation source is also one of the main causes of the degradation process. It acts as a catalyst, enhancing the speed of some chemical reactions and breaking chemical bonds (mainly C-H and C-O) of the materials. Moreover, it accelerates the oxidation, darkening and yellowing of binders, catalyzing radical oxidation reactions in proteinaceous binders or affecting the amide bonds [12] and favoring the cleavage of fatty acid chains in lipidic ones [13,14]. Numerous studies have been already carried out by subjecting synthetic painted samples to UV radiation in order to simulate accelerated ageing procedures in closed environments [15–17]. Some of them have even applied UV-B light (280–315 nm) as radiation source, instead of the most common one for these treatments, UV-A (315–400 nm) to study the ageing effect in the stability of different acrylic binding media [18].

For the characterization of color and chemical properties of artwork, several analytical techniques can be employed [3,19]. Among them, Fiber Optics Reflectance Spectroscopy (FORS), Raman spectroscopy, X-Ray Fluorescence (XRF) or gas chromatography (GC) are commonly used for this purpose, either alone or in combination in the form of multi-analytical approaches [20–22]. Infrared spectroscopy has also a great potential in this field, being suitable for the identification of both organic and inorganic pigments and binders [23,24]. The technique is particularly useful for the characterization of organic materials in artworks [25], including studies on changes induced by UV radiation exposure. Thus, the interaction of binders and pigments of different nature [26] and the kinetic of the photodegradation of natural resins acting as varnishes [27] have been previously studied by means of IR spectroscopy.

Hyperspectral imaging (HSI) is an active area of research that has grown quickly during the last decade. It collects information from three dimensions – two spatial (x, y) and one spectral (λ), resulting in a (x, y, λ) dataset which is typically referred to as a datacube. The term hyperspectral refers to the collection of a large number of spectral channels, usually more than 100, in comparison with multi-spectral [28]. Thereby, HSI exhibits more sensitivity to subtle spectral variations. In the last years, there has been an increasing interest in the use of non-invasive macroscopic HSI for the study of artworks [29–31]. Most studies have focused on the use of reflectance spectroscopy in the visible range for pigment identification with improved results by extending into the NIR range [32–34]. Although it is experimentally much more complex, remote-sensing HSI in the mid-IR has also been reported [35].

On the other hand, by integrating HSI with microscopy into one system, hyperspectral microscope imaging (HMI) techniques can collect spectral information with spatial resolution at the microscopic level. This is also an interesting tool for artworks examination since factors affecting the macroscopic appearance of an artwork, like color, texture or sheen, are typically controlled by phenomena occurring at the microscale (such as changes in oxidation state or grain size/shape) that may be studied using microimaging techniques. The study of features at the microscale usually involved sampling and preparation of cross-sections to provide information about the underlying structure, chemistry, and stratigraphy of objects [22,36]. In this work, we propose the use of this methodology for the characterization of the molecular changes taking place in binders and pigments of varied hues and nature during consecutive steps of an UV ageing procedure. Instead of using cross-sections, we propose the investigation of intact model samples in the reflection mode. In this way, the technique would be suitable for the investigation of intact artefacts or fragments of a suitable size to fit into the microscope measurement plate. Using hyperspectral micro-FTIR imaging and chemometrics we will achieve information about how UV radiation induces changes in pigments and binders, taking also into account the sample heterogeneities typical of paintings (like layer thickness, pigment particle size, local differences in binder/pigment ratio, surface texture, etc.). Complementary measurements by means of colorimetry (FORS) and optical microscopy help to describe the macroscopic changes in color.

## 2. Materials and methods

### 2.1. Samples preparation

Two identical plaster plates (20 × 15 cm) were prepared to be used as a reference and main mock-up for the ageing experiments. Four different pigments: vermilion (HgS), orpiment ($As_2S_3$), azurite ($Cu_3(CO_3)_2(OH)_2$) and lead white ($(PbCO_3)_2$ $Pb(OH)_2$); and three binders: rabbit glue, egg tempera and linseed oil, were considered.

Pigments were purchased from Kremer Pigmente GmbH & Co. KG (Germany) in the form of powder. Binders were acquired from local stores and prepared as follows. Linseed oil was used in its raw form. Granular rabbit glue (5 g) was immersed in 50 mL of distilled water for 24 h, for the particles to swell up. Then, the remaining water was boiled and re-used to dissolve the rabbit glue. For the egg tempera binder, a yolk was mixed with two drops of linseed oil and two drops of distilled water and stirred into a homogenous mixture.

The painting mixtures (pigment-binder) were all prepared in individual plastic containers, by mixing 0,2500 g of pigment and the necessary amount of binder (3:1 proportion). Fifteen model samples were prepared by painting the plaster plates. The platters were dried for a month at room temperature and in a dark environment before starting the artificial ageing with UV light.

### 2.2. Instrumentation

#### 2.2.1. Ageing approach

A SwiftCure HL250 UV radiation ageing chamber was used for the simulation of the accelerated ageing procedure of the samples. The platters are located in a sealed cell inside an irradiation chamber (UV-A 315–400 nm: 30 W and UV-B 280–315 nm: 3 W). Three cycles of time were considered (24 h, 72 h and 120 h) maintaining them at 35 °C ± 0,6°C by means of a water bath temperature control system. Samples without any sort of ageing treatment were used for the reference measurements (0 h).

*2.2.2. Sample characterization*

For the visual inspection, a Dino Lite optical microscope equipped with a polarized light regulator was employed. Visible images of the surface of the samples were taken by using 15X, 100X and 200X magnification. Reflectance measurements in the range between 400 and 700 nm were carried out by means of a compact and portable Bluewave-Vis spectrometer (StellarNet) equipped with a charge-coupled detector and employing a tungsten-krypton lamp and an optical fiber probe (600 μm internal diameter). The measurement was performed by keeping the probe at 90° with respect to the sample, which is illuminated over a surface area of ca. 4 $mm^2$ at a distance of 15 mm. A 50 mm Halon reflectance standard (STN-RS50) was used as a reference, registering its spectrum in the same conditions. Colorimetric parameters were calculated using the CIELAB system, namely L* for the lightness, a*, from green (-) to red (+), and b*, from blue (-) to yellow (+) [37]. Total color parameter ΔE*ab (eq. (1), [38]) was used to show the overall color variation of samples during the ageing procedure:

$$\Delta E^{*}_{ab} = \sqrt{(L_2 - L_1)^2 + (b_2 + b_1)^2 + (a_2 - a_1)^2} \quad (1)$$

It has been calculated for each step of the ageing process, being L1, b1 and a1 those parameters corresponding to 0 h of UV exposure.

FT-IR hyperspectral images were obtained with a Jasco Fourier transform infrared (FTIR) 6300 spectrometer coupled to an FTIR IRT-7000 microscope equipped with a single element mercury cadmium telluride (MCT) detector and a XYZ automated stage for mapping. A 16X Cassegrain objective (20 mm distance work) working in reflection mode was used to focus the infrared beam on the sample and to collect the radiation reflected. An adjustable aperture allowed data collection from a localized spatial position within the sample with desired spatial dimensions. We used the point to point scanning method, in which the sample is scanned by moving the sample stage and recording a spectrum corresponding to a small area at a time [39]. In this way, each spectrum recorded corresponds to a pixel of the image. The aperture size was optimized to 100 μm × 100 μm in order to achieve good signal-to-noise ratio. We recorded maps of 1,5 mm × 1,5 mm total size consisting of 225 spectra registered in the range between 3100 and 800 $cm^{-1}$ with a spectral resolution of 4 $cm^{-1}$. Each spectrum was average of 200 scans and, therefore, each map recording lasted around 100 min. The same area of each sample was considered for the successive maps acquisition after UV treatment. To be sure, they were marked for simple visual identification. The background was always acquired in a clean area of the plaster plate.

*2.2.3. Data analysis*

Infrared spectra were pre-processed by an area-normalization. Selected spectral ranges were employed for each binder depending on characteristic spectral changes, being 2000–1400 $cm^{-1}$, 3100–1000 $cm^{-1}$ and 2000–1000 $cm^{-1}$ for rabbit glue, linseed oil and egg tempera, respectively. PCA Model Editor 2.12.00 from Spectra Manager version 2 (JASCO) was used to build the principal component analysis models. A cross-validation procedure based on leave one out method was used in order to evaluate the performance of the models. Micro Spectra Analysis software (JASCO) was used to obtain different ratios of both peak intensities or areas to construct false color images.

## 3. Results

In this work, the evolution of binders and pigments during ageing in model plaster samples has been studied in order to get information about the chemical changes occurring through degradation under UV exposition. The set of mock-up samples with different combinations of pigments and binders was prepared using a plaster plate as support, taking into account the importance of gypsum in historical paintings. Gypsum has not only been utilized as the support element itself, like in the case of Muslim or Islamic plasterwork coatings [19,21], but it is also commonly employed as a preparation layer for priming purposes on wooden, wall painting or canvas supports [40].

Samples were exposed to four-time cycles of UV radiation under temperature-controlled conditions (35 °C ± 0,6°C), employing a continuous cooling current, as already reported by Tochácek *et al.* [41]. A detailed characterization of the aged samples was carried out by means of several optical and spectroscopic techniques exploiting the use of hyperspectral images after each of those time cycles.

*3.1. Visual and colorimetric impact of ageing*

The progressive loss of color is one of the early indications of the deterioration process in paintings and polychromies. Exposition to UV radiation can accelerate that effect. This can be observed in the microscopic images, being particularly evident in the case of orpiment (not shown). The total color parameter (ΔE*ab) reflects the global changes in the color of the samples during the ageing process as shown in Fig. 1. The changes were analyzed considering also the corresponding CIELab* spaces containing a* and b* color parameters (Figure S1, Supplementary information) and reflectance spectra depicted in Fig. 2.

Color changes related to ageing appear to be very dependent on both the pigment and the binder. In general, the color was more stable when using egg tempera, especially for vermilion, whereas all the pigments, except white lead, showed the highest color changes when using rabbit glue as binder. The pigments vermilion and orpiment suffered the highest variations, with ΔE*ab values up to 52 and 41, respectively, while color changes for azurite and lead white were less pronounced (maximum ΔE*ab of 26 and 15, respectively). This is in agreement with previous knowledge about photostability of these pigments [42]. The visual inspection of the microscopic images showed that orpiment is coarser-grained than vermilion, which can favour certain detachment, besides decoloration. For orpiment, parameter b* (yellow factor) drastically decreases upon ageing, being especially noticeable in the case of rabbit skin glue and linseed oil. This can also be seen in the reflectance spectra, in which the band around 435 nm shows a much smaller curvature at 120 h of UV treatment. In previous studies [42], orpiment has been reported to become paler and colourless on exposure to light as it converts to arsenic oxide (arsenolite, $As_2O_3$). The minimum in the reflectance spectra of vermilion samples appears close to 600 nm, showing a much less broad absorbance band with increasing irradiation time with rabbit glue and linseed oil. This is reflected in the decreasing of both a* and b* color parameters. Azurite owes its blue color to a combination of d-d and charge transfer absorptions [43]. In its reflectance spectra, a prominent maximum located at 475 nm appears and, as it can be observed, it is less pronounced in those samples of advanced ageing state. This is particularly accused when linseed oil acts as the binder. This change is reflected in a progressive decrease of CIELab* parameter -b* (blue indicator) with UV exposure and it could be considered the initiation of the typical yellowing observed in many oil-based paintings due to binder oxidation [27]. In the case of lead white samples, there are no significant changes in neither reflectance spectra nor colorimetric parameters throughout the process. It is observed a certain decrease of the parameter a*, particularly noticeable for egg tempera, and probably related to the loss of the yellow color of the binders (especially egg yolk), more perceptible when mixed with this white pigment.

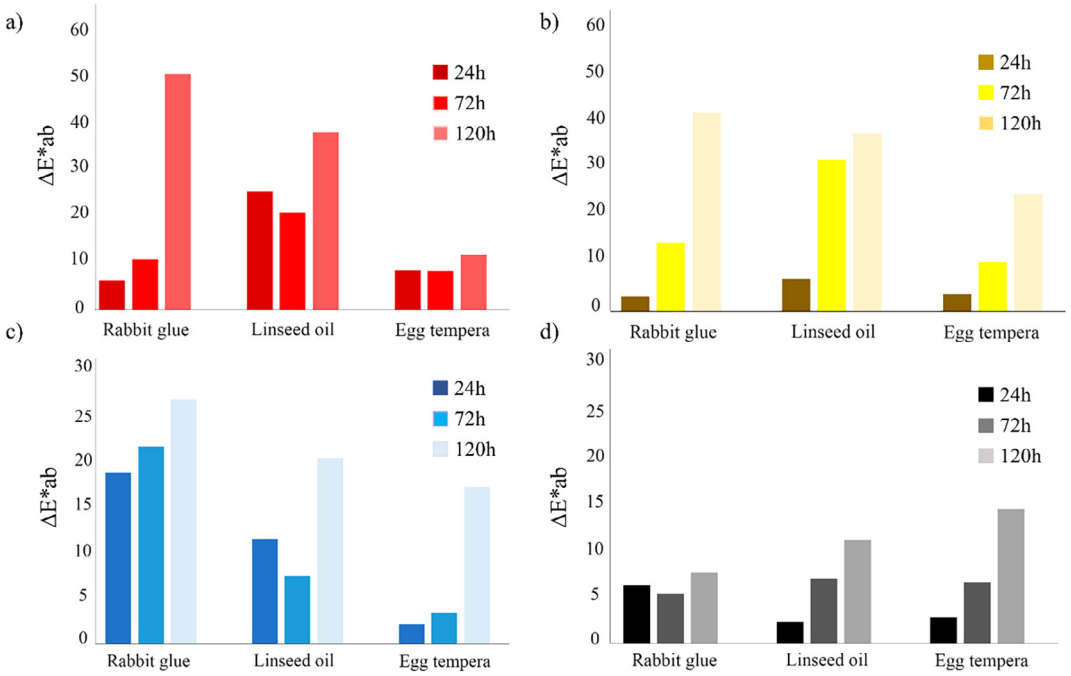


**Fig. 1.** Graphs representing changes of ΔE*ab (total color parameter) of (a) vermilion, (b) orpiment, (c) azurite and (d) lead white samples painted with rabbit glue, linseed oil and egg tempera binders through UV accelerated ageing procedure.

Regarding CIElab* parameter L*, an increase during the exposition treatment has been observed in most cases, as can be expected from the loss of color. Vermilion samples (especially when painted with rabbit glue and egg tempera) experienced a growth of more than 20% from 0 h to 120 h states. A similar situation can be detected for azurite samples, which increases up to 75%. For orpiment, the initial L* values were already very high (close to 70%) and ended up to 90%, being particularly remarkable the mixture with rabbit glue, reaching values up to 93%.

### 3.2. IR microspectroscopic characterization

In order to investigate spectral changes taking place during the consecutive steps of the ageing process, FTIR hyperspectral images of all the samples were recorded after each of the UV exposition cycles. First, the main spectral features of the pure binders and binder-pigments mixtures will be discussed before considering UV-induced changes. In Fig. 3, single spectra of the binders and the mixtures are displayed, showing the initial state of the process (0 h of ageing treatment). To interpret these FTIR spectra obtained in reflection mode, it is necessary to take into account the appearance of distortions with respect to the spectra acquired in the transmission mode. Furthermore, since the sample surface is not optically flat, both diffuse and specular reflected light are collected in unknown proportions, impeding any mathematical correction. Thus, some distortions appear as derivative-like spectral features and inverted bands, following the Reststrahlen effect. In addition, sometimes overtones and combination bands increase their signals because many reflections occur.

For the rabbit skin glue samples, the most intense bands of the binder are in agreement with those reported by Manfredi et al. [40] and can be attributed to strong absorptions of C=O stretching in amide I (1695 $cm^{-1}$) and amide II (around 1577 $cm^{-1}$) involving CN stretching and NH bending. An additional feature is observed at 1472 $cm^{-1}$ which can be assigned to $CH_2$ scissoring modes. When the binder is mixed with the pigments, these spectral features are sometimes hidden under bands of azurite and lead white. In the case of vermilion and orpiment, the binder absorptions dominate the spectrum since $As_2S_3$ and HgS do not present spectral features in the mid-infrared region. Here, the typical bands of rabbit skin glue appear broadened and clearly shifted to lower wavenumbers (1650, 1548 and 1457 $cm^{-1}$). The observed shift can reflect changes in protein secondary structure and/or hydrogen bonding on hydration sites such as C=O and N-H upon interaction with the pigments. Additionally, other optical effects can be considered for the explanation of these shifts. The mixing with the pigments probably enhances diffuse reflected radiation and dismisses the proportion of specularly reflected components.

In the un-treated linseed oil spectra, bands located at 2930 $cm^{-1}$ and 2855 $cm^{-1}$ are assigned to asymmetric and symmetric (C—H) $CH_2$ stretching [44], as well as the small shoulder at 1463 $cm^{-1}$, related to $sp^3$ C-H bending vibration [45]. The most intense band appearing at 1742 $cm^{-1}$ is attributed to the C=O ester vibration. The typical band of the olefinic C-H stretching at 3010 $cm^{-1}$, characteristic of unconjugated cis double bonds is not observed. This reflects the complete drying of oil film during the month after applying it, which involves several processes as cis–trans isomerization, conjugation, oxidation and polymerization, all of them responsible for the depletion of this band [46,47].

Furthermore, the sharp features observed at 1684 $cm^{-1}$ and 1630 $cm^{-1}$, as well as the inverted band observed at about 1152 $cm^{-1}$ do not correspond to the characteristic bands of the binder. In fact, they can be attributed to gypsum bands of the plaster plate. The first two can be assigned to the deformation vibrations of the O–H bond of the water molecules of the gypsum (see Figure S2, Supplementary information).

Moreover, due to the high adsorption index k, the asymmetric $SO_4^{2-}$ stretching band of gypsum is affected by the Reststrahlen effect and consequently appears as an inverted band. These bands were not observable in the spectra of the binders containing proteins (rabbit skin glue and egg tempera), due to the strong absorption of the amide I bands. Bands characteristic of the binder are slightly shifted in the mixtures with pigments with respect to the pure binder but in lees extension as for rabbit skin glue. This

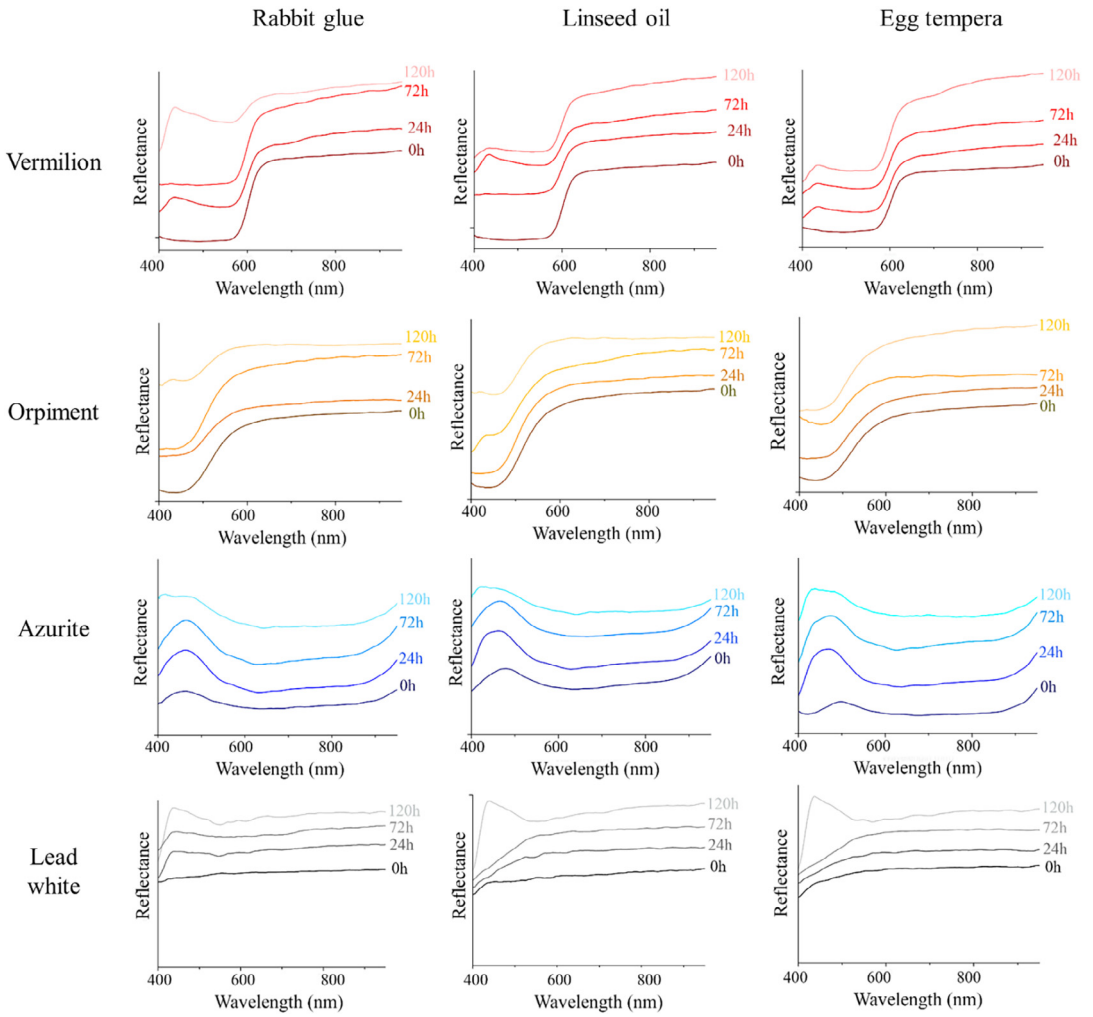


**Fig. 2.** Reflectance spectra of pigments when rabbit glue, linseed oil and egg tempera are employed as binders. Color code for the figure: **O** = Orpiment, **V** = Vermilion, **A** = Azurite and **W** = lead white. Spectra were stacked for better visualization.

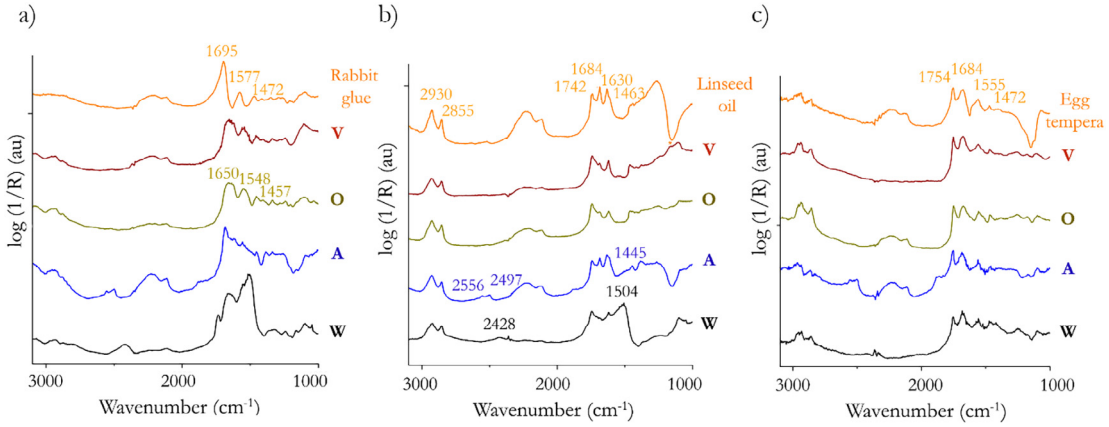


**Fig. 3.** Infrared spectra of (a) rabbit glue, (b) linseed oil and (c) egg tempera samples at the initial state (0 h) of the ageing process. Color code for the figure: **O** = Orpiment, **V** = Vermilion, **A** = Azurite, **W** = lead white. Spectra were stacked for better visualization.

shifts are indicative of pigment-binder interaction as pointed out in other studies [48].

Regarding egg tempera, the two bands situated at 1754 $cm^{-1}$ and 1684 $cm^{-1}$ correspond to C=O stretching of the lipidic part of the binder and C=O stretching of amide I (protein), respectively. The band related to the absorption of amide II can be found at 1555 $cm^{-1}$ and the band appearing around 1470 $cm^{-1}$ can be attributed to bending asymmetric vibrations of $CH_3$ [49].

When considering the spectra of the pigments, only azurite and white lead show characteristic bands in the spectral region under

investigation. Their spectral features are more easily identified in the mixture with linseed oil. Thus, for lead white, the distorted Reststrahlen band of antisymmetric $CO_3^{2-}$ stretching (ν3) can be observed between 1392 $cm^{-1}$ and 1504 $cm^{-1}$ and the combination band of ν1 + ν3 at about 2428 $cm^{-1}$ due to the $((PbCO_3)_2.Pb(OH)_2)$ structure of hydrocerussite [40,50]. In the case of azurite, spectral features coincide with those previously reported for its reflection infrared spectra, which shows strong absorptions in the region between 1450 and 1420 $cm^{-1}$, related to the ν3 of $CO_3^{2-}$. There are also two bands located at 2497 $cm^{-1}$ and 2556 $cm^{-1}$ due to ν1 + ν3 combination.

In order to study the changes induced by the accelerated UV ageing, we have used FTIR hyperspectral images, as they contain large amounts of information since each pixel corresponds to an infrared spectrum. Painting layers are intrinsically heterogeneous, for example on thickness or pigment-binder distribution, and this may influence the behaviour upon UV irradiation. The use of hyperspectral micro-images enables to take into consideration these sample heterogeneities. Thus, using hyperspectral micro-images each pixel of the image can be considered as a "sample replicate" under the same irradiation conditions, providing a statistically more robust approach for the evaluation of the changes induced by irradiation in comparison with the conventional approach (an average FT-IR spectrum acquired on each sample). To deal with this large amount of information the use of chemometric tools is mandatory. Here, we used principal component analysis (PCA) to extract the information embodied in the hyperspectral data. In this way, we identified maximum variance within the multivariate data space. The PCA results have been interpreted by investigating simultaneously the scores and loading plots. For each binder, we have compared the results considering the binder alone (single-binder models, all summarized in Fig. 4) and mixed with the different pigments (pigment-binder models). Furthermore, models combining different pigments with the same binder (two pigment-binder models) were investigated to study the influence of the pigment identity in the changes. The following discussion will be organized according to the binder employed.

### 3.2.1. Rabbit skin glue

Fig. 4a shows the results of PC analysis for the samples considering the rabbit glue alone. Taking into account that no pretreatment of the spectra was considered, PC1 (99,1%) reflects the average values of all spectra, and it is necessary to consider the PC4 (0,38%) to find the changes related to the irradiation. The variability collected by PC2 and PC3, not related to UV-irradiation time, is possibly explained by differences in the proportion of specular reflected radiation, since this binder showed the brightest surface. The inspection of the loading of PC4 revealed a shift in the band of the Amide I, with a decrease of the component at higher wavenumber (1755 $cm^{-1}$) and the increase of the lower wavenumber side of the band (1693 $cm^{-1}$). This is in agreement with former studies that reported the shifting of amide bands of collagen upon UV irradiation due to the induced disorder of the secondary structure [51]. When studying the pigment-binder models, the tendency is similar, being particularly clear in the case of orpiment and vermillion, thus no effects due to the identity of the pigment were observed. Interestingly, additional features at 1770 and 1724 $cm^{-1}$ increase with ageing. This is also observed in models combining data from two different pigments with the same binder, as it is the case for vermilion and orpiment. Since these two pigments do not present spectral features in the mid-IR region, the data have been treated

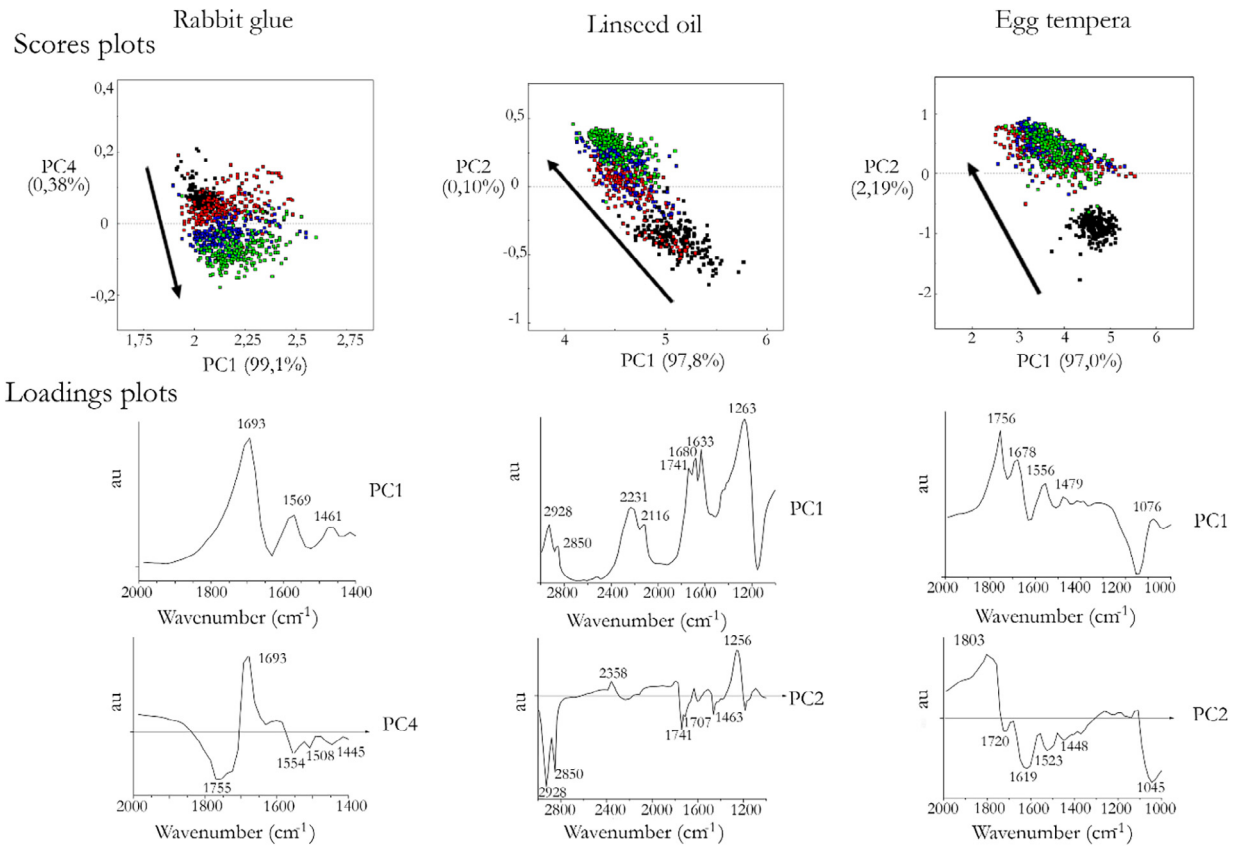


**Fig. 4.** Single-binder PCA models for rabbit glue, linseed oil and egg tempera including score graphs and more relevant loadings plots. Color code for the score plots: 0 h (black), 24 h (red), 72 h (blue) and 120 h (green).

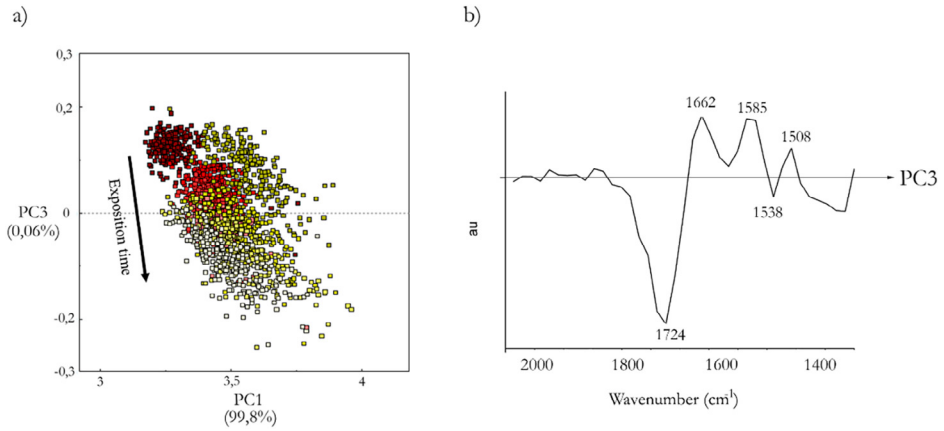


**Fig. 5.** Two pigments-binder PCA model for vermilion (red) and orpiment (yellow) samples with rabbit skin glue including (a) score graph and (b) more relevant loadings plot. Color code for the score plot: from dark to bright color (0 h to 120 h). Arrow to indicate the direction from initial to final step of ageing treatment.

together building a two pigments-binder PCA model (see Fig. 5). As can be seen, there is a clear grouping of the spectra according to the irradiation time along the axis defined by PC3. It exhibits a progression from untreated samples (dark red and yellow for vermilion and orpiment, respectively) owing positive score values, to samples at 120 h of the ageing procedure, showing negative values in this case and labelled with light colors.

The band at 1724 $cm^{-1}$, which increases with irradiation time, can be attributed to carbonyl moieties formed by oxidation of the proteins. This seems to indicate that the presence of pigments favored the degradation of proteins. This is most remarkable in the case of orpiment, with larger changes in PC3 score values. The oxidation of the polypeptidic chains leading to the generation of carbonyl compounds with characteristic vibrations in the region 1700–1750 $cm^{-1}$ has been previously described for degraded historical parchments [52]. In fact, the increase of the intensity of this region with respect to the Amide I band has been proposed as a marker for oxidative damage of parchments. In Fig. 6, the ratio of the intensities of 1724 $cm^{-1}$ and 1649 $cm^{-1}$ bands for the vermilion sample is shown. As can be observed, the band related to carbonyl moieties starts increasing its intensity in relation to the Amide I band at the very first stages of the ageing treatment, reaching high values at the end of the treatment. This means it can be described as a gradual process, happening along with the UV exposure time.

### 3.2.2. Linseed oil

In the case of linseed oil, the changes observed for the binder alone revealed a general decrease in its characteristic bands (2928, 2850, 1742, 1710, 1463 and 1182 $cm^{-1}$) upon UV irradiation, as can be seen in the loading plot of PC2 (0,10%) in Fig. 4. This can be attributed to certain evaporation of the organic medium due to the breakdown of the triacylglycerols and the formation of volatile compounds.

This can be further illustrated (see Fig. 7) by constructing distribution maps showing the ratio between the area of the main band of linseed oil (1742 $cm^{-1}$) and the most intense band of the gypsum support (1684 $cm^{-1}$) during the ageing process. The proportion of linseed oil clearly decreases with irradiation time.

This effect is not observed when the pigments are added to the binder, which is in agreement with previous studies based on thermogravimetric analysis (TG) and gas chromatography-mass spectrometry (GC–MS) [53]. These authors observed that when fatty acids were saponified by the $Pb^{2+}$ present in the lead white pigment, the evaporation of the binder did not take place, in contrast with the surprisingly fast rate of depletion of glycerol and fatty acids for the binder alone upon ageing. In our case, when the binder was mixed with pigments, the inspection of loading and score plots for each pigment revealed certain distinctive features (see Table 1).

Changes upon irradiation were more easily observed for vermilion and orpiment, as explained before. Azurite showed the most complex pattern of changes and the tendencies with irradiation were more difficult to interpret. In general, the broadening of the carbonyl band with ageing, which had been observed in previous studies [46–49], was revealed to be due to the increase of bands in the region 1790–1770 $cm^{-1}$ and 1710–1670 $cm^{-1}$. The exact positions of the bands were dependent on the pigment identity. The band at ~ 1780 $cm^{-1}$ can be assigned to lactones or anhydrides. This absorption is thought to be specific for drying oils [47]. The absorption at 1710–1690 $cm^{-1}$ can be assigned to the carboxylic and dicarboxylic acids (like azelaic acid) typically formed upon oxi-

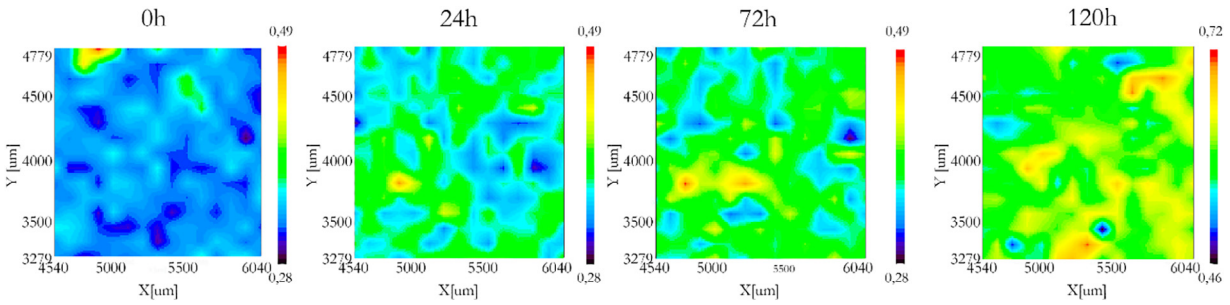


**Fig. 6.** False-color distribution maps of the spatial distribution of the ratio of the intensities at 1724 $cm^{-1}$/ 1649 $cm^{-1}$ of vermilion pigment with rabbit skin glue binder obtained at the progressive stages of the ageing process.

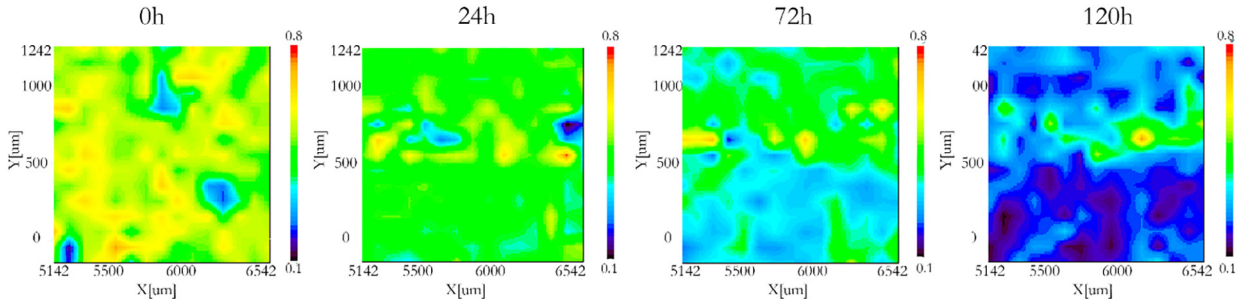


**Fig. 7.** False-color distribution maps of the spatial distribution of the ratio of the areas of 1742 $cm^{-1}$/1684 $cm^{-1}$ of linseed oil sample of the plaster plate obtained at the progressive stages of the ageing process.

**Table 1**
Tentative assignment of changes in the infrared bands during ageing of samples with different pigments and linseed oil as binder.

| Pigment | Bands ($cm^{-1}$) | | Assignment | Reference |
|---|---|---|---|---|
| Vermilion | Increasing | 1770 | C=O stretching of ester | [45] |
| | | 1701 | Carboxylic and dicarboxylic acids | [47] |
| | | 1616 | Formation of calcium oxalates | [54] |
| | Decreasing | 1187 | C—O stretching of triglycerides | [53] |
| Orpiment | Increasing | 1772 | C=O stretching of ester | [45] |
| | | 1677 | Conjugated carbonyl compounds | [53] |
| | | 1629 | Calcium oxalates | [54] |
| | Decreasing | 1741 | C=O stretching of ester | [45] |
| | | 1146 | C-O stretching of triglycerides | [53] |
| Azurite | Increasing | 2558 | ν1 + ν3 combination modes of $CO_3^{2-}$ of pigment | [48] |
| | | 2496 | ν1 + ν3 combination modes of $CO_3^{2-}$ of pigment | [48] |
| | | 1879 | ν1 + ν4 combination modes of $CO_3^{2-}$ of pigment | [48] |
| | | 1587 | Copper carboxylates | [53] |
| | Decreasing | 1741 | C=O stretching of ester | [45] |
| | | 1689 | Conjugated carbonyl compounds | [53] |
| | | 1463 | Antisymmetric stretching (ν3) of $CO_3^{2-}$ of pigment | [48] |
| | | 1432 | Antisymmetric stretching (ν3) of $CO_3^{2-}$ of pigment | [48] |
| White lead | Increasing | 1787 | Lactones or anhydrides | [47] |
| | | 1725 | ν1 + ν4 combination modes of $CO_3^{2-}$ of pigment | [48] |
| | | 1494 | Antisymmetric stretching (ν3) of $CO_3^{2-}$ of pigment | [39] |
| | Decreasing | 2913 | Asymmetric (C—H) $CH_2$ stretching | [44] |
| | | 2853 | Symmetric (C—H) $CH_2$ stretching | [44] |
| | | 1679 | Conjugated carbonyl compounds | [53] |
| | | 1509 | Lead carboxylates | [53] |
| | | 1125 | C—O stretching of triglycerides | [53] |

dation. Features at lower wavenumbers like 1670 $cm^{-1}$ can be attributed to conjugated carbonyl compounds. In all cases, a decrease of the intensity in the region 1190–1120 $cm^{-1}$ (attributed to C-O stretching of triglycerides) was also observed. Furthermore, the formation of metal carboxylates has been reported to be a common degradation phenomenon in paintings, due to the reaction of mono and dicarboxylic acids not incorporated in the polyanionic network with metal cations from the pigments. In our study, this was clearly observed only for azurite, with the increase of the band at 1587 $cm^{-1}$ characteristic of copper carboxylates [54]. In the case of lead white, the band at 1509 $cm^{-1}$ observed in the loading vector of the PC related to ageing, is difficult to attribute to lead carboxylates, as the pigment shows a band in the region. For vermillion and orpiment, there was no evidence of metal carboxylates formation. Nevertheless, the increasing band observed for these two pigments at ca. 1620 $cm^{-1}$ could be attributed to calcium oxalates formed due to the interaction of oxalic acid, a dicarboxylic acid typically found in aged lipidic binders [55], and the gypsum support.

*3.2.3. Egg tempera*

In the case of this binder, the score plot of PC1 versus PC2 for the single binder PCA model (Fig. 4) shows a clear distinction between the non-irradiated samples (0 h) and the rest, corresponding to the progressive steps of the ageing process. This reveals that main changes occurred during the first hours of irradiation. The same happened for the pigment-binder models, which is an interesting observation since, for this binder, the color changes of the pigments occurred in the opposite way: little color changes were detected at the beginning and they were more pronounced with long exposure times. Thus, in the initial phases of the ageing treatment, the oxidation of the binder was the main effect induced by UV irradiation. This fact was particularly remarkable in the case of lead white (see Fig. 8). This suggests that the presence of lead white accelerated the oxidation of the binder. In the case of azurite, the tendency observed is more complex, since the score values for PC2 increase in the first steps of irradiation and then decrease reaching negative values. The inspection of the corresponding loading vectors revealed changes mostly coincident with those observed for linseed oil. The most noticeable were the increase of absorption bands at 1770 $cm^{-1}$ and 1710 $cm^{-1}$. This is not surprising since egg tempera is a mixture of egg yolk and linseed oil, and triglycerides are present in both materials. The distinctive features of egg yolk are the bands of proteins, which seem to be more stable upon irradiation than lipidic components. As can be seen in Fig. 8, in the case of this binder, it is also remarkable that the changes associated with irradiation are clearly reflected in changes in the score values of more than one PC (with the exception of vermilion, for which PC2 explained most of the variance related to ageing).

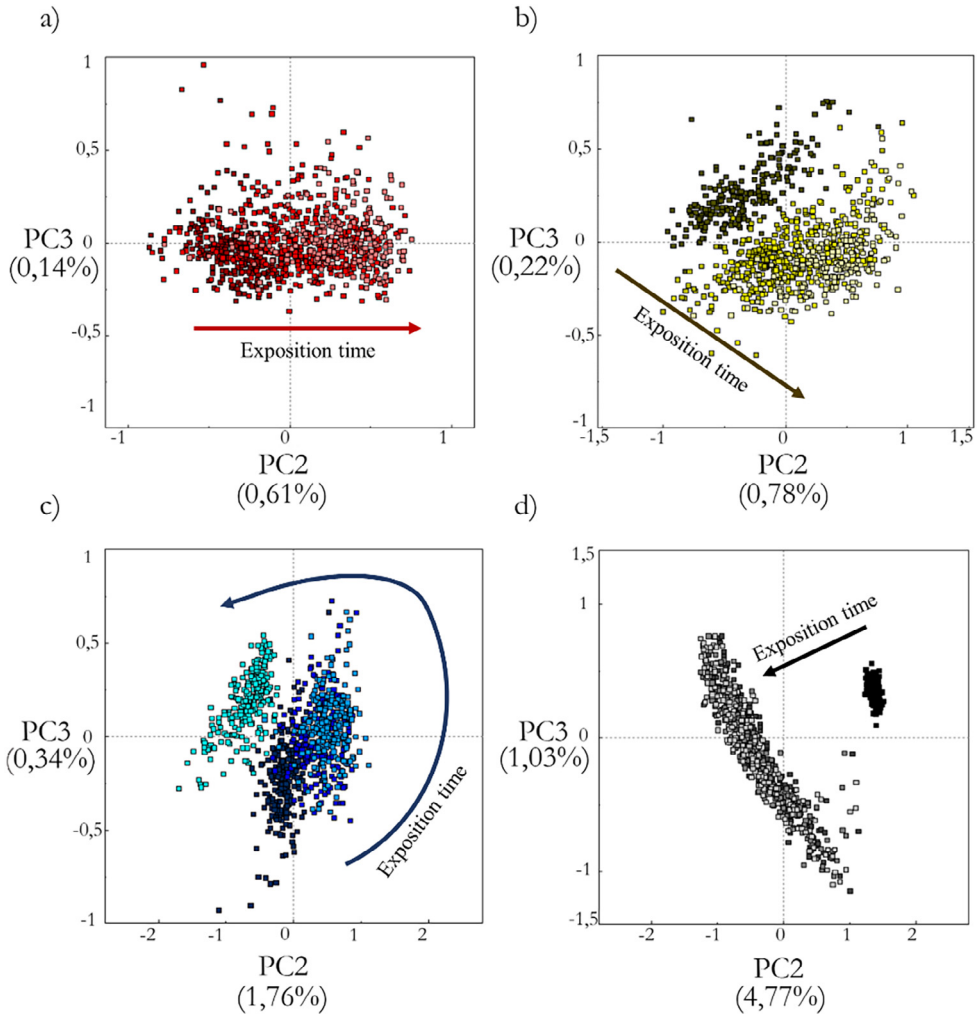


**Fig. 8.** Score plots of pigment-binder PCA models of (a) vermilion, (b) orpiment, (c) azurite and (d) lead white with egg tempera. Color code for the figure: from dark to bright color (0 h to 120 h). Arrows to indicate the direction from initial to final step of ageing treatment.

Since principal components are mutually orthogonal that means that two uncorrelated processes are simultaneously happening upon irradiation. The inspection of the loadings of PC2 and PC3 revealed differences mainly in the region 1200–1100 $cm^{-1}$. They could be related to the oxidation of phospholipids present in egg yolk that present distinctive spectral features in this region when compared with triglycerides [56].

## 4. Conclusions

The methodological study presented illustrates the high potential of hyperspectral infrared microimaging for the investigation of UV induced changes of organic binders in pictorial layers. Painting layers are intrinsically heterogeneous, showing variable thickness and surface roughness and with uneven pigment-binder distribution. Using FTIR microimaging each pixel of the image is representative of the sample area of the mock-up sample from it was recorded and therefore, when the whole image is considered, differences in the behaviour upon UV irradiation are taken into consideration. To extract useful information from the data, different PCA models have been built including both single-binder models and models with pigment-binder mixtures. Even when considering short UV radiation exposition times, the characteristic spectral changes of the binders have been detected, being mostly related to the formation of oxidized functional groups. Fiber optic visible reflection spectroscopy (FORS) provided complementary information about the color changes of the pigments. However, no clear relation was found between colorimetric changes registered and the alteration processes suffered by the binders in our model samples. The interaction between different pigments and binders is also an interesting issue. Thus, for example, in the case of egg tempera, it was clearly seen that the presence of lead accelerated the alteration of the binder and this was also reflected in the loss of the yellow color due to the binder in these mixtures. Curiously, for the rest of the analyzed pigments, egg tempera seemed to play a protective role in the preservation of the color. The obtained results highlight the need of considering pigment-binder interactions when studying the degradation processes of the binders. This is the case, for example of linseed oil: the evaporation of the binder, probably due to the breakdown of the triacylglycerols, was clearly observed in the single binder model but not when it was mixed with the pigments. Even when more investigations are needed to draw general conclusions on the effects of different pigments on a given binder, the usefulness of hyperspectral FTIR microimaging for the evaluation of UV induced ageing of pictorial samples is demonstrated.

## Declaration of Competing Interest

The authors declare that they have no known competing financial interests or personal relationships that could have appeared to influence the work reported in this paper.

## Acknowledgments

This work was financed with the project BIA2017-87131-R (Spanish Ministry of Economy, Industry and Competitiveness). Authors would also like to acknowledge technical and financial support from FQM-363 Research group and CICT of the Universidad de Jaén. M. González-Cabrera also acknowledges the FPU15/03119 fellowship from Spanish Ministry of Education, Culture and Sport.

## References

[1] M.A. Rogerio-Candelera, M. Lazzari, E. Cano, Science and Technology for the Conservation of Cultural Heritage, Taylor & Francis, United Kingdom, 2013.
[2] A. Heritage, S. Golfomitsou, Conservation science: Reflections and future perspectives, Stud. Conserv. 60 (2015) S22–S26.
[3] J.M. Madariaga, Analytical chemistry in the field of cultural heritage, Anal. Meth. 7 (2015) 4848–4876.
[4] T. Aytürk, A History of the Restoration and Conservation of Works of Art - Alessandro Conti, Electa, Florence, 1998.
[5] A. Nevin, Pigment Alteration, in: Encycl. Archaeol. Sci., John Wiley & Sons, Inc., Hoboken, NJ, USA, 2018: pp. 1–4.
[6] R.L. Feller, Aspects of chemical research in conservation: The deterioration process, J. Am. Inst. Conserv. 33 (1994) 91–99.
[7] Y.M. Issa, G. Abdel-Maksoud, M. Ibrahim, M. Magdy, A combination of analytical methods to evaluate the effect of humidity aging on the painting materials of icon models, Vib. Spectrosc. 107 (2020) 103010.
[8] F. Modugno, F. Di Gianvincenzo, I. Degano, I.D. van der Werf, I. Bonaduce, K.J. van den Berg, On the influence of relative humidity on the oxidation and hydrolysis of fresh and aged oil paints, Sci. Rep. 9 (2019) 1–16.
[9] S. Garrappa, E. Kočí, S. Švarcová, P. Bezdička, D. Hradil, Initial stages of metal soaps' formation in model paints: The role of humidity, Microchem. J. 156 (2020) 104842.
[10] J.S. Mills, R. White, The organic chemistry of museum objects, Butterworth-Heinemann Series Conservat. Museol. (1987).
[11] X. Martiarena, Conservación y restauración, Cuad. Sección. Artes Plásticas y Doc. 10 (1992) 177–224.
[12] E. Manzano, N. Navas, R. Checa-Moreno, L. Rodriguez-Simón, L.F. Capitán-Vallvey, Preliminary study of UV ageing process of proteinaceous paint binder by FT-IR and principal component analysis, Talanta 77 (2009) 1724–1731.
[13] M.P. Colombini, F. Modugno, R. Fuoco, A. Tognazzi, A GC-MS study on the deterioration of lipidic paint binders, Microchem. J. 73 (2002) 175–185.
[14] E.J. Llorent-Martínez, A. Domínguez-Vidal, R. Rubio-Domene, M.I. Pascual-Reguera, A. Ruiz-Medina, M.J. Ayora-Cañada, Identification of lipidic binding media in plasterwork decorations from the Alhambra using GC-MS and chemometrics: Influence of pigments and aging, Microchem. J. 115 (2014) 11–18.
[15] K. Elert, C. Cardell, Weathering behavior of cinnabar-based tempera paints upon natural and accelerated aging, Spectrochim, Acta Part A Mol. Biomol. Spectrosc. 216 (2019) 236–248.
[16] P.M. Whitmore, V.G. Colaluca, The natural and accelerated aging of an acrylic artists' medium, Stud. Conserv. 40 (1995) 51–64.
[17] T. Learner, O. Chiantore, D.M. Scalarone, Ageing studies on acrylic emulsion paints, Prepr, ICOM Comm. Conserv. 13th Trienn. Meet. James James. (2002) 911–919.
[18] V. Pintus, S. Wei, M. Schreiner, Accelerated UV ageing studies of acrylic, alkyd, and polyvinyl acetate paints: Influence of inorganic pigments, Microchem. J. 124 (2016) 949–961.
[19] F.J. Collado-Montero, A.I. Calero-Castillo, M. Melgosa, V.J. Medina, Colorimetric Evaluation of Pictorial Coatings in Conservation of Plasterworks from the Islamic Tradition, Stud. Conserv. 64 (2019) 90–100.
[20] M. Picollo, M. Bacci, A. Casini, F. Lotti, S. Porcinai, B. Radicati, L. Stefani, Fiber Optics Reflectance Spectroscopy: A Non-destructive Technique for the Analysis of Works of Art, in: Opt. Sensors Microsystems, Kluwer Academic Publishers, Netherlands, 2005: 259–265.
[21] P. Arjonilla, M.J. Ayora-Cañada, R. Rubio Domene, E. Correa Gómez, M.J. de la Torre-López, A. Domínguez-Vidal, Romantic restorations in the Alhambra monument: Spectroscopic characterization of decorative plasterwork in the Royal Baths of Comares, J. Raman Spectrosc. 50 (2019) 184–192.
[22] S. Sotiropoulou, G. Sciutto, A.L. Tenorio, J. Mazurek, I. Bonaduce, S. Prati, R. Mazzeo, M. Schilling, M.P. Colombini, Advanced analytical investigation on degradation markers in wall paintings, Microchem. J. 139 (2018) 278–294.
[23] E.L. Kendix, S. Prati, R. Mazzeo, E. Joseph, G. Sciutto, C. Fagnano, Far Infrared spectroscopy in the field of cultural heritage, E-PRESERVATIONScience. 7 (2010) 8–13.
[24] K. Katayama, H. Kandori, FTIR study of primate color visual pigments, Biophys. 11 (2015) 61–66.
[25] F. Rosi, A. Daveri, C. Miliani, G. Verri, P. Benedetti, F. Piqué, B.G. Brunetti, A. Sgamellotti, Non-invasive identification of organic materials in wall paintings by fiber optic reflectance infrared spectroscopy: A statistical multivariate approach, Anal. Bioanal. Chem. 395 (2009) 2097–2106.
[26] D. Pellegrini, C. Duce, I. Bonaduce, S. Biagi, L. Ghezzi, M.P. Colombini, M.R. Tinè, E. Bramanti, Fourier transform infrared spectroscopic study of rabbit glue/inorganic pigments mixtures in fresh and aged reference paint reconstructions, Microchem. J. 124 (2016) 31–35.
[27] C. Azémard, C. Vieillescazes, M. Ménager, Effect of photodegradation on the identification of natural varnishes by FT-IR spectroscopy, Microchem. J. 112 (2014) 137–149.
[28] H. Grahn, P. Geladi, Techniques and applications of hyperspectral image analysis, J, Wiley, 2007.
[29] C. Fischer, I. Kakoulli, Multispectral and hyperspectral imaging technologies in conservation: current research and potential applications, Stud. Conserv. 51 (2006) 3–16.
[30] C. Cucci, J.K. Delaney, M. Picollo, Reflectance Hyperspectral Imaging for Investigation of Works of Art: Old Master Paintings and Illuminated Manuscripts, Acc. Chem. Res. 49 (2016) 2070–2079.
[31] M. Picollo, C. Cucci, A. Casini, L. Stefani, Hyper-spectral imaging technique in the cultural heritage field: New possible scenarios, Sensors. 20 (2020) 2843.
[32] J.K. Delaney, J.G. Zeibel, M. Thoury, R. Littleton, M. Palmer, K.M. Morales, E.R. De La Rie, A. Hoenigswald, Visible and infrared imaging spectroscopy of picasso's harlequin musician: Mapping and identification of artist materials in situ, Appl. Spectrosc. 64 (2010) 584–594.
[33] C. Biron, A. Mounier, G. Le Bourdon, L. Servant, R. Chapoulie, F. Daniel, A blue can conceal another! Noninvasive multispectroscopic analyses of mixtures of indigo and Prussian blue, Color Res. Appl. 45 (2020) 262–274.
[34] L. de Viguerie, N.O. Pladevall, H. Lotz, V. Freni, N. Fauquet, M. Mestre, P. Walter, M. Verdaguer, Mapping pigments and binders in 15th century Gothic works of art using a combination of visible and near infrared hyperspectral imaging, Microchem. J. 155 (2020) 104674.
[35] F. Rosi, C. Miliani, R. Braun, R. Harig, D. Sali, B.G. Brunetti, A. Sgamellotti, Noninvasive Analysis of Paintings by Mid-infrared Hyperspectral Imaging, Angew. Chemie Int. Ed. 52 (2013) 5258–5261.
[36] F. Rosi, A. Federici, B.G. Brunetti, A. Sgamellotti, S. Clementi, C. Miliani, Multivariate chemical mapping of pigments and binders in easel painting cross-sections by micro IR reflection spectroscopy, Anal. Bioanal. Chem. 399 (2011) 3133–3145.
[37] Hunter Lab, CIE L*a*b* Color Scale. Insight on color, Apl. Note. 8 (1996).
[38] D.H. Brainard, Color Appearance and Color Difference Specification, Optical Society of America, Washington, 2003.
[39] J. Sellors, R.A. Crocombe, R.A. Holt, N.A. Wright, FT-IR Imaging Hardware, in: S. Sasic, Y. Ozaki (Eds.), Raman, Infrared, Wiley, Near-Infrared Chem. Imaging, 2010.
[40] M. Manfredi, E. Barberis, A. Rava, E. Robotti, F. Gosetti, E. Marengo, Portable diffuse reflectance infrared Fourier transform (DRIFT) technique for the non-invasive identification of canvas ground: IR spectra reference collection, Anal. Meth. 7 (2015) 2313–2322.
[41] J. Tocháček, Z. Vrátníčková, Polymer life-time prediction: The role of temperature in UV accelerated ageing of polypropylene and its copolymers, Polym. Test. 36 (2014) 82–87.
[42] A. Coccato, L. Moens, P. Vandenabeele, On the stability of mediaeval inorganic pigments: A literature review of the effect of climate, material selection, biological activity, analysis and conservation treatments, Herit. Sci. 5 (2017) 12.
[43] R.L. Feller, Artists' Pigments: a handbook of their history and characteristics, Washington D.C, National Gallery of Art, 1993.
[44] Z. Rahiminezhad, H. Hashemi Gahruie, S. Esteghlal, G.R. Mesbahi, M.T. Golmakani, S.M.H. Hosseini, Oxidative stability of linseed oil nano-emulsions filled in calcium alginate hydrogels, LWT. 127 (2020) 109392.
[45] S. Lang, Q. Zhou, Synthesis and characterization of poly(urea-formaldehyde) microcapsules containing linseed oil for self-healing coating development, Prog. Org. Coatings. 105 (2017) 99–110.
[46] B. Muik, B. Lendl, A. Molina-Diaz, M. Valcarcel, M.J. Ayora-Cañada, Two-dimensional correlation spectroscopy and multivariate curve resolution for the study of lipid oxidation in edible oils monitored by FTIR and FT-Raman spectroscopy, Anal. Chim. Acta 593 (2007) 54–67.
[47] R.J. Meilunas, J.G. Bentsen, A. Steinberg, Analysis of Aged Paint Binders by FTIR Spectroscopy, Stud. Conserv. 35 (1990) 33–51.
[48] I.A. Balakhnina, N.N. Brandt, Y.S. Kimberg, N.L. Rebrikova, A.Y. Chikishev, Variations in the IR spectra of yellow ochre due to mixing with binding medium and drying, J. Appl. Spectrosc. 78 (2011) 183–188.
[49] J. van der Weerd, A. van Loon, J.J. Boon, FTIR studies of the effects of pigments on the aging of oil, Stud. Conserv. 50 (2005) 3–22.
[50] C. Miliani, F. Rosi, A. Daveri, B.G. Brunetti, Reflection infrared spectroscopy for the non-invasive in situ study of artists' pigments, Appl. Phys. A Mater. Sci. Process. 106 (2012) 295–307.
[51] A. Kamińska, A. Sionkowska, Effect of UV radiation on the infrared spectra of collagen, Polym. Degrad. Stab. 51 (1996) 19–26.
[52] M. Ciglanská, V. Jančovičová, B. Havlínová, Z. Machatová, V. Brezová, The influence of pollutants on accelerated ageing of parchment with iron gall inks, J. Cult. Herit. 15 (2014) 373–381.
[53] I. Bonaduce, L. Carlyle, M.P. Colombini, C. Duce, C. Ferrari, E. Ribechini, P. Selleri, M.R. Tiné, New Insights into the Ageing of Linseed Oil Paint Binder: A Qualitative and Quantitative Analytical Study, PLoS One 7 (2012) e49333.
[54] V. Otero, D. Sanches, C. Montagner, M. Vilarigues, L. Carlyle, J.A. Lopes, M.J. Melo, Characterisation of metal carboxylates by Raman and infrared spectroscopy in works of art, J. Raman Spectrosc. 45 (2014) 1197–1206.

[55] M.P. Colombini, F. Modugno, E. Menicagli, R. Fuoco, A. Giacomelli, GC-MS characterization of proteinaceous and lipid binders in UV aged polychrome artifacts, Microchem. J. 67 (2000) 291–300.

[56] J.M. Nzai, A. Proctor, Determination of phospholipids in vegetable oil by fourier transform infrared spectroscopy, JAOCS, J. Am. Oil Chem. Soc. 75 (1998) 1281–1289.